HOKKAIDO UNIVERSITY

Title	The fabrication of Ni quantum cross devices with a 17 nm junction and their current-voltage characteristics
Author(s)	Kaiju, Hideo; Kondo, Kenji; Ono, Akito et al.
Citation	Nanotechnology, 21(1), 015301 https://doi.org/10.1088/0957-4484/21/1/015301
Issue Date	2010-01-08
Doc URL	https://hdl.handle.net/2115/49333
Rights	This is an author-created, un-copyedited version of an article accepted for publication in Nanotechnology. IOP Publishing Ltd is not responsible for any errors or omissions in this version of the manuscript or any version derived from it. The definitive publisher authenticated version is available online at 10.1088/0957-4484/21/1/015301
Type	journal article
File Information	Nan21-1_015301.pdf

Hokkaido University Collection of Scholarly and Academic Papers : HUSCAP

Nanotechnology **21**, 015301 (2010)

Fabrication of Ni quantum cross devices with a 17-nm-size junction and its current-voltage characteristics

Hideo Kaiju[1,2], Kenji Kondo[1], Akito Ono[1], Nobuyoshi Kawaguchi[1], Jonghan Won[3], Akihiko Hirata[3], Manabu Ishimaru[3], Yoshihiko Hirotsu[3] and Akira Ishibashi[1]

[1] Research Institute for Electronic Science, Hokkaido University, Sapporo, Hokkaido 001-0020, Japan
[2] PRESTO, Japan Science and Technology Agency (JST), Kawaguchi, Saitama 332-0012, Japan
[3] The Institute of Scientific and Industrial Research, Osaka University, Ibaraki, Osaka 567-0047, Japan

E-mail: kaiju@es.hokudai.ac.jp

Abstract. Quantum cross (QC) devices which consist of two Ni thin films deposited on polyethylene naphthalate (PEN) substrates with their edges crossing have been fabricated and its current-voltage characteristics have been investigated. The cross-sectional area between the two Ni electrodes, which was made without the use of electron-beam or optical lithography, is as small as 17 nm x 17 nm. We have successfully obtained ohmic current-voltage characteristics, which show good agreement with calculation results within the framework of modified Anderson model. The calculated results also predict a high switching ratio in excess of 100000:1 for QC devices having the molecule sandwiched between the Ni electrodes. This indicates that QC devices having the molecule can be expected to have potential application in novel switching devices.

1. Introduction

To fabricate nanoscale patterns with the sub-10-nm feature size has been an important research target for potential applications in the next-generation memories, microprocessors, logic devices and other novel functional devices. Typically, according to the International Technology Roadmap for Semiconductor (ITRS) in 2008, an 11-nm node device is targeted for the year 2022 [1]. To achieve this milestone, liquid immersion lithography and extreme ultraviolet (EUV) lithography can be expected as the most commonly used technique for the fabrication of nanopatterns. Liquid immersion lithography using a wavelength of 193 nm has demonstrated that 32-nm features can be patterned [2]. EUV lithography using a short wavelength of 13.5 nm enabled the printing of nearly 27-nm half-pitch lines [3].

On the other hand, attractive patterning techniques, such as multi-step nanoimprint lithography (NIL), a mold-to-mold cross imprint (MTMCI) process and a surface sol-gel process combined with photolithography, are currently proposed and pursued actively as an alternative patterning method [4-7]. Multi-step NIL using a mold produced by the spatial frequency doubling method has achieved the

production of 17-nm line width patterning [4,5]. The MTMCI process using silicon nanowires formed by spacer lithography, in which nanoscale line features are defined by the residual of a conformal film on the edges of a sacrificial support structure with the line width controlled by the film thickness, has produced a large array of 30 nm wide silicon nanopillars [6]. The surface sol-gel process combined with photolithography, where the line width is determined by the thickness of coating silica layer on the resist pattern, has achieved the size reduction and proliferation of sub-20-nm silica wall [7].

Recently, we have proposed a double nano-*baumkuchen* (DNB) structure, in which two thin slices of alternating metal/insulator nano-*baumkuchen* are attached so that the metal/insulator stripe is crossing each other, as a lithography-free nanostructure fabrication technology [8]. The schematic illustration of the fabrication procedure has been reported in our previous paper [9]. Utilizing this DNB structure, we can expect to realize high-density memory devices, the cross point of which can be scaled down to ultimate feature sizes of a few nanometers thanks to the film thickness determined by the metal-deposition rate, ranging from 0.01 to 1 nm/s. One element of the DNB structure is called a quantum cross (QC) device that consists of two metal nanoribbons having the edge-to-edge configuration [9-11]. When molecular-based self-assembled monolayers (SAMs) [12-14], such as rotaxanes, catenanes and pseudorotaxanes, are sandwiched between the two thin metal ribbons, QC devices can serve as novel non-volatile memory devices and switching devices. Moreover, when magnetic materials, such as Fe, Co, and Ni, are used for the two metal nanoribbons, QC devices can work as nanoscale spin injectors and tunneling magnetoresistance (TMR) devices.

In this paper, toward the realization of DNB structures, we have fabricated QC devices using Ni thin films on polyethylene naphthalate (PEN) organic substrates and investigated the current-voltage characteristics. We have also reported the calculation results of the electronic transport for QC devices with the molecule sandwiched between the Ni film edges.

2. Experiments

2.1. Fabrication of quantum cross devices

Fabrication method of quantum cross devices is shown in figure 1. First, Ni thin films were thermally evaporated on PEN substrates (2 mm width, 10 mm length and 100 μm thickness) in a high vacuum chamber at the base pressure of ~10^{-8} torr. PEN films TEONEX Q65 were supplied by Teijin DuPont Japan and cut down from 5 to 2 mm width using a slitter in a clean environment. The pressure during the evaporation was 10^{-5} torr and the temperature near PEN substrates was less than 62 °C, which was lower than the glass transition temperature T_g of 120 °C for PEN substrates. The growth rate was 0.93 nm/min at the evaporation power of 280 W.

Then, Fabricated Ni/PEN films were sandwiched between two polymethyl methacrylate (PMMA) resins using epoxy. The size of the PMMA resin was 6 mm x 6 mm x 3 mm. The edge of PMMA/Ni/PEN/PMMA was polished by chemical mechanical polishing (CMP) methods using alumina (Al_2O_3) slurries with a particle diameter of 0.1, 0.3 and 1.0 μm. The polishing pressure was

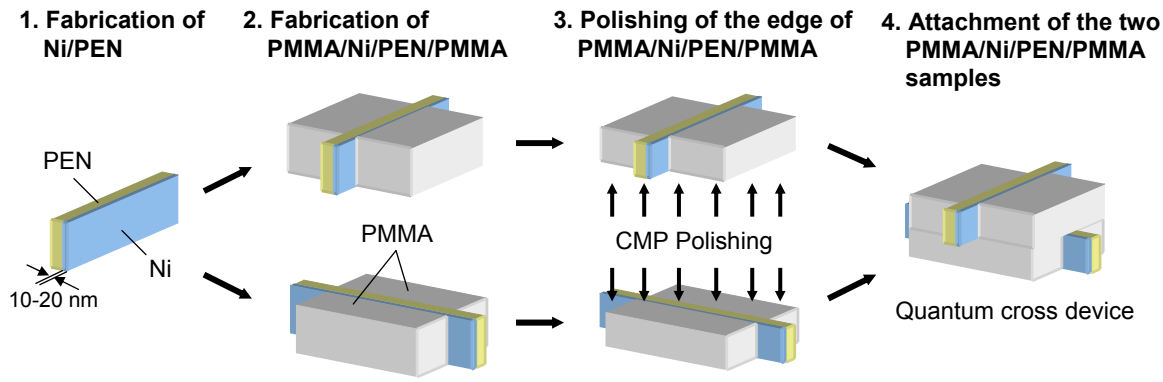


Figure 1. Fabrication method of quantum cross devices.

6.5 psi and the platen rotation speed was 75 rpm. Finally, Two sets of polished PMMA/Ni/PEN/PMMA were prepared and attached together with their edges crossing in a highly clean environment of ISO class minus 1 [15]. The attachment pressure was 0.54 MPa and no glue was used. The fabricated QC device is shown in figure 1.

2.2. Evaluation of Ni/PEN films and quantum cross devices

The Ni thickness was measured by a mechanical method using the stylus surface profiler DEKTAK and an optical method using the diode pumped solid state (DPSS) green laser and the photo diode detector. The surface morphologies of Ni/PEN samples were analyzed by atomic force microscope (AFM) Nanoscope IIIa. The microstructures as well as the Ni/PEN interfacial structures were examined using a JEOL JEM-3000F transmission electron microscope (TEM) operating at 300 kV. The cross-sectional TEM samples were prepared by a combination of mechanical polishing and Ar ion thinning. To reduce the beam-heating effects during ion thinning, the sample stage was cooled to -160 ^{o}C by liquid nitrogen conduction cooling. The current-voltage characteristics of QC devices were measured by a four-probe method at room temperature.

3. Results and discussion

3.1. Cross-sectional TEM image of Ni/PEN films

Figure 2(a) shows the cross-sectional TEM image for Ni (20 nm)/PEN films. It can be found that there is no diffusion of Ni into the PEN layer, resulting in clear and smooth formation of the Ni/PEN interface. Here, it should be noted that some researchers have reported that metal atoms diffuse into organic layers in the process of the metal evaporation onto organic layers [16-18]. For example, the metastable atom electron spectroscopy (MAES) spectra of Au on the p-sexiphenyl (6P)/Au system shows that the features of 6P remain even though Au was deposited to about 20 nm thickness. This indicates that Au atoms or clusters penetrate into the 6P films [16]. The soft x-ray photoemission spectroscopy (SXPS) investigation of the interface between evaporated indium and perylenetetracarboxylic dianhydride (PTCDA) also demonstrates that the interfacial region is very wide ranging from 7 to 60 nm and it means that the metal atoms of indium diffuse into perylenetetracarboxylic dianhydride (PTCDA) organic layers [17]. Moreover, according to studies on the interaction between evaporated Ag and octadecanethiol (ODT) on Au films using XPS, Ag deposited at 300 K migrates through the octadecanethiol (ODT) layer and resides at the ODT/Au interface [18]. For comparison, such a metal diffusion into organic layers does not occur in Ni/PEN interface. This indicates that Ni thin films on PEN organic substrates are suitable for metal/organic films of QC devices. It can be also confirmed that the surface of Ni films is smooth, and this

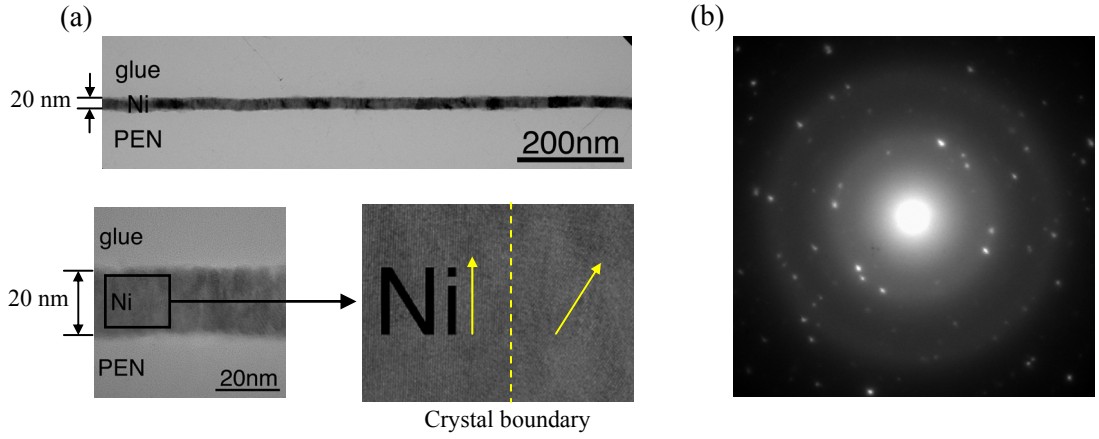


Figure 2. (a) Cross-sectional TEM image and (b) ED pattern for Ni (20 nm)/PEN films.

smoothness is in good agreement with the results of the AFM observation, where the surface roughness R_a is 1.1 nm.

Figure 2(b) shows the ED pattern for the same specimen. Ni thin films on PEN films have face-centered-cubic (FCC) structures, which are equal to those in bulk Ni structures. ED pattern also shows that Ni thin films have polycrystalline structures, which can be recognized from the cross-sectional TEM image of figure 2(a), where one can see the crystal boundary clearly. The ring patterns have not been observed although the probe size to take this diffraction pattern is 50-100 nm. This indicates that the Ni crystalline size is large, and as estimated from the contrast of the cross-sectional TEM image in figure 2(a), the crystalline size is found to be 20-50 nm. Here, as we consider the feasibility for QC devices, the large crystalline is good for QC devices. This is because the edge-surface structure of the junction has the same crystal orientation when the crystalline size is larger than the film thickness. Therefore, Ni/PEN films are suitable for QC devices from a viewpoint of the Ni/PEN interfacial structures and the crystalline size of Ni films.

3.2. AFM Surface morphology of Ni/PEN films

Figure 3(a) shows the AFM surface morphology for PEN, where the scanning area is 1×1 μm^2. The surface roughness R_a is 1.3 nm, which is a very small value for organic films. Figure 3(b) shows the AFM surface morphology for Ni(16 nm)/PEN. The surface roughness R_a of 1.1 nm is obtained, and it indicates that a smooth surface is formed for metal thin films on organic substrates. Figure 3(c) shows the surface morphology for Au(14 nm)/PEN. The surface roughness R_a is 3.1 nm. It is found that the surface roughness is changed by metal films even though the same PEN films are used as a substrate. Here, we consider the feasibility for QC devices from a viewpoint of the scaling dependence of the

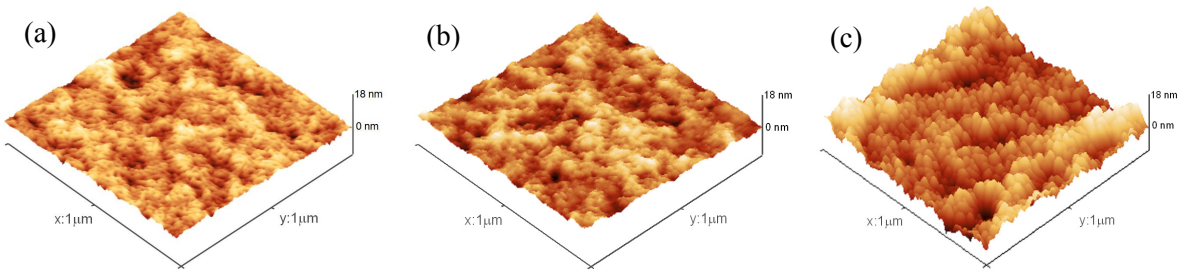


Figure 3. AFM surface morphology for (a) PEN, (b) Ni(16 nm)/PEN and (c) Au(14 nm)/PEN.

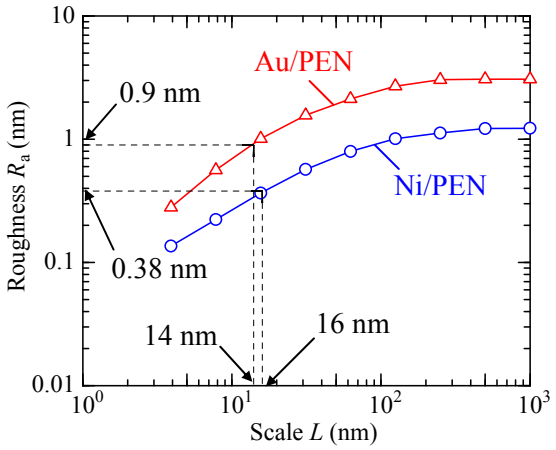


Figure 4. Scanning scale dependence of the surface roughness for Ni/PEN and Au/PEN.

surface roughness. In QC devices, the crossing area determined by film thickness is so important that it is necessary to investigate the surface roughness in the same scanning size as the thickness. The scanning size dependence of the surface roughness for Ni/PEN and Au/PEN is shown in figure 4. With the decrease of the scanning size, the surface roughness decreases for each sample. For Au(14 nm)/PEN, the surface roughness is 0.9 nm, which corresponds to 4-5 atomic layers, in the scanning size of 14 nm. In contrast, for Ni(16 nm)/PEN, the surface roughness is 0.38 nm, which corresponds to 2 atomic layers, in the scanning size of 16 nm. These experimental results show that Ni/PEN films are suitable for QC devices from a viewpoint of the scaling properties of surface roughness in addition to the Ni/PEN interfacial structures and the crystalline size of Ni films mentioned above.

3.3 Current-voltage characteristics of quantum cross devices

Figure 5 shows the current-voltage characteristics for QC devices using Ni/PEN films. The inset shows the experimental setup for the four-probe method. Since the Ni thickness is 17 nm, the cross-sectional area between two Ni thin films is 17 nm x 17 nm. As seen from figure 5, the ohmic current-voltage characteristics have been obtained for both the positive and negative bias at room temperature. Figure 6 shows the aging properties for the voltage with a constant current of 0.1, 0.2, 0.3, 0.5, 0.7 and 1.0 μA, respectively. The voltage is stable in any current and the standard deviation of the voltage is 22-25 mV, which corresponds to the signal-to-noise (SN) ratio of 34-52 dB, where the SN ratio is

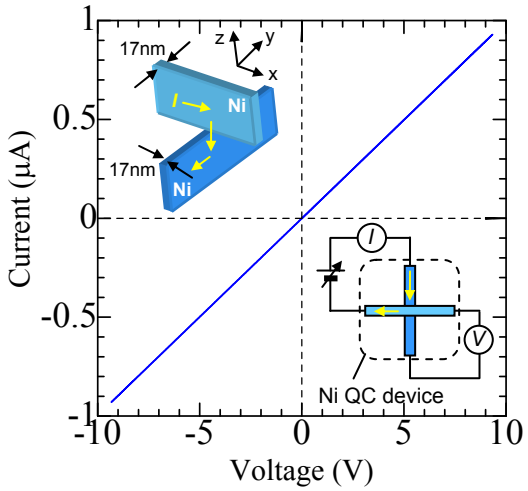


Figure 5. Current-voltage characteristics for Ni QC devices with a 17-nm-size junction.

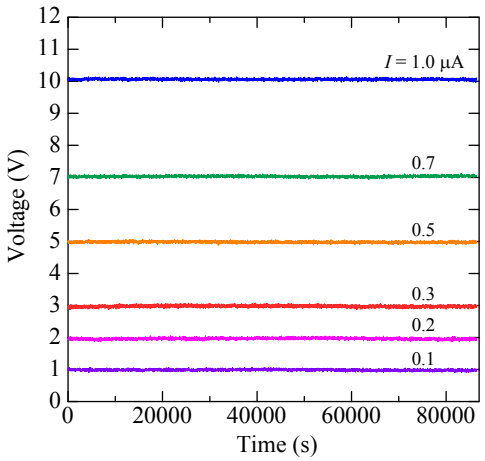


Figure 6. Aging properties for QC devices using Ni(17 nm)/PEN films.

defined by $20\lg V/\Delta V$. Here, it should be noted that the fabrication of nano-junctions using the film edges had been challenged by other researchers before [19]. According to their attempts, Co and Ni thin films were evaporated on glass substrates using vacuum evaporation and then they were cleaved and stuck to each other with their edges crossing. Although the current flowed across the junction, there had remained a few problems that the edge angle had to be 15-25^{o} inclined and the film thickness had to be larger than 50 nm. Furthermore, the current was slightly changed as time passed although the current flowed. In contrast, such problems have not been occurred in our experiments, and we have obtained stable ohmic characteristics, where there has been no change with time, for the 17-nm-size junction. These experimental results indicate that our method using thin film edges can be expected as a new nanostructure fabrication technology beyond conventional lithography.

3.4 Calculated current-voltage characteristics of quantum cross devices with the molecule

Finally, we show the theoretical calculation results for current-voltage characteristics of QC devices with the molecule. In the calculation model, we assume that the molecule having some energy levels is sandwiched between the two edges of Ni films. The calculation has been performed within the framework of modified Anderson model, where the Anderson Hamiltonian is given by

$$H = H_{\text{electrodes}} + H_{\text{mole}} + H_{\text{t}}. \tag{1}$$

Here, $H_{\text{electrodes}}$ is the Hamiltonian of both the Ni electrodes, H_{mole} is the Hamiltonian of the molecule sandwiched between both the Ni electrodes, and H_{t} is the transfer Hamiltonian between the sandwiched molecule and each Ni electrode. $H_{\text{electrodes}}$, H_{mole} and H_{t} can be expressed by

$$\begin{aligned} H_{\text{electrodes}} &= \sum_{\alpha=T,B}\sum_{k,\sigma}\varepsilon_{k\sigma}c^{+}_{\alpha,k\sigma}c_{\alpha,k\sigma}, \\ H_{\text{mole}} &= \sum_{i,\sigma}\varepsilon_0(i)\,a^{+}_{i,\sigma}a_{i,\sigma}, \\ H_{\text{t}} &= \sum_{\alpha=T,B}\sum_{k,\sigma}\sum_{i,\sigma}(V_\alpha c^{+}_{\alpha,k\sigma}a_{i,\sigma} + h.c.). \end{aligned} \tag{2}$$

Here, $\varepsilon_{k\sigma}$ is the free electron energy of $\hbar^2k^2/2m$, where m is the free electron mass, $\hbar$ is the Planck's constant and k is a two-dimensional wave number. $c^{+}_{\alpha,k\sigma}$ and $c_{\alpha,k\sigma}$ are creation and annihilation operators for electrons of wave number k and spin index σ in α electrode. α indicates the top or bottom Ni electrode. $\varepsilon_0(i)$ represents the i-th energy level of eigen-states of the molecule. $a^{+}_{i,\sigma}$ and $a_{i,\sigma}$ are creation and annihilation operators for electrons of spin index σ in the i-th energy level of the molecule. The N (= 2) energy levels in the molecule are assumed to be $\varepsilon_0(1) = 0.5\,\text{eV}$ and $\varepsilon_0(2) = 1\,\text{eV}$, respectively. V_α is the transfer matrix between the molecule and α electrode. As we derive the current flowing from the top to bottom Ni electrode for QC devices using these equations, we can obtain

$$I = \frac{2e^2}{h}\int_{E_{\text{F}}}^{E_{\text{F}}+eV} d\varepsilon \sum_i \left(\frac{4\Gamma_{\text{T}}(\varepsilon)\Gamma_{\text{B}}(\varepsilon)}{(\varepsilon-\varepsilon_0(i))^2 + (\Gamma_{\text{T}}(\varepsilon)+\Gamma_{\text{B}}(\varepsilon))^2} \right) [f(\varepsilon - eV - E_{\text{F}}) - f(\varepsilon - E_{\text{F}})], \tag{3}$$

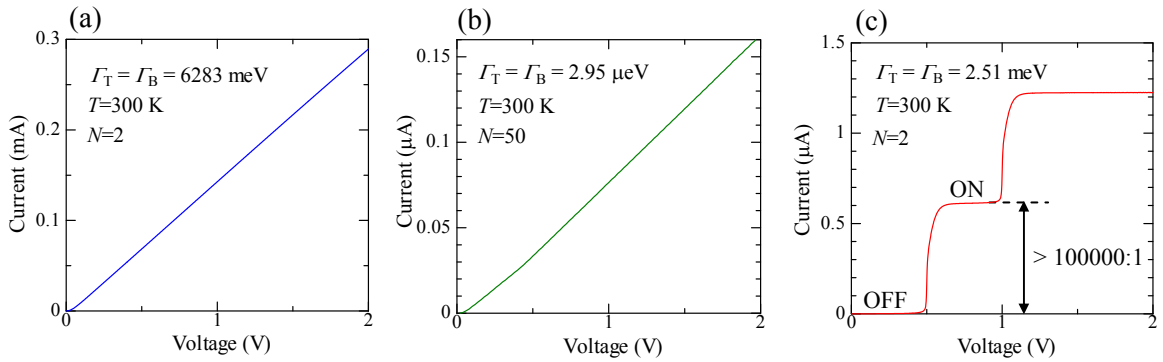


Figure 7. Calculated current-voltage characteristics for QC devices under the (a) strong coupling limit and the number of the energy levels N=2, (b) weak coupling condition and N=50, and (c) weak coupling condition and N=2.

where e is the elementary charge, E_F is the Fermi energy of Ni, and $f(\varepsilon)$ is the Fermi-Dirac distribution function [11]. $\Gamma_{T(B)}(\varepsilon)$ is the coupling strength between the top (bottom) Ni electrode and the sandwiched material, which is given by

$$\Gamma_{T(B)}(\varepsilon) = \pi D_{T(B)}(\varepsilon) |V_{T(B)}|^2 , \quad (4)$$

where $D_{T(B)}(\varepsilon)$ is a density of states of electrons for the top (bottom) Ni electrode and $V_{T(B)}$ is the coupling constant between the top (bottom) Ni electrode and the sandwiched material. These coupling strengths correspond to the broadening of the energy level of the sandwiched material induced by the interaction with itinerant electrons in each electrode. The situation of $\Gamma_{T(B)}(\varepsilon) >> k_B T$, where k_B is the Boltzmann constant and T is the ambient temperature of 26 meV, is defined as the strong coupling limit, and the situation of $\Gamma_{T(B)}(\varepsilon) < k_B T$ is defined as the weak coupling condition. The strong coupling limit indicates that the top Ni electrode directly contacts with the bottom Ni electrode. Figure 7(a) shows the calculated current-voltage characteristics for QC devices under the strong coupling limit. The coupling constant $V_{T(B)}$ is assumed to be 10.0 meV, corresponding to the coupling strengths $\Gamma_{T(B)}(\varepsilon)$ of 6283 meV. We have obtained the ohmic current-voltage characteristics, which are in good agreement with the experimental results shown in figure 5, qualitatively. However, the calculation results are not in quantitative agreement with the experimental results, especially in terms of the resistance. Then, we consider another calculation condition, where the N (= 50) energy levels in the junction are assumed to be $\varepsilon_0(1)$ = 0.04 eV, $\varepsilon_0(2)$ = 0.08 eV, …. , and $\varepsilon_0(50)$ = 2.0 eV, and the coupling constant $V_{T(B)}$ is assumed to be 0.015 meV, which corresponds to the coupling strength $\Gamma_{T(B)}(\varepsilon)$ of 2.95 μeV. This situation means that the top Ni electrode contacts with the bottom Ni electrode under the weak coupling. The calculated current-voltage characteristics are shown in figure 7(b). We have obtained the ohmic current-voltage characteristics, where the resistance is ~MΩ. These calculation results show quantitative agreement with experimental results.

Figure 7(c) shows the calculated current-voltage characteristics of QC devices under the weak coupling condition and the number of the energy levels N=2. The coupling constant $V_{T(B)}$ is 0.2 meV, corresponding to the coupling strengths $\Gamma_{T(B)}(\varepsilon)$ of 2.51 meV. This situation means that the molecule is sandwiched between the two Ni electrodes. From figure 7(c), the calculated result shows the sharp steps at the positions of the energy level of the sandwiched molecule. The off-state current I_0 is 0.57 pA at the voltage V_0 of 0.006 V, and the on-state current I_1 is 0.59 μA at the voltage V_1 of 0.6 V. As we estimate the switching on/off ratio, the I_1/I_0 ratio is found to be an excess of 100000:1. Here, it should be noted that it is essentially important that the junction area is as small as nanometer-size in order to obtain such a high on/off ratio. When the junction area is as large as sub-micrometer-size, the number of the molecule sandwiched between the electrodes is large, so the energy level can be broadening. In contrast, when the junction area is as small as nanometer-size, the number of the molecule is small, so the energy level can be discrete. This discrete energy level leads to the sharp steps in the current-voltage characteristics, which can produce such a high switching ratio. These results indicate that QC devices having the molecule can be expected to have potential application in novel switching devices. Therefore, the nanostructure fabrication method using thin film edges, proposed in this paper, is a great important technology in terms of not only to exceed the limitation of lithography but also to create new switching devices with an ultrahigh on/off ratio.

4. Conclusion

We have fabricated a quantum cross (QC) device which consists of two Ni thin films deposited on polyethylene naphthalate (PEN) substrates with their edges crossing. Since the thickness of Ni films was 17 nm, the cross-sectional area was as small as 17 nm x 17 nm, which was produced without the use of electron-beam or optical lithography. We have successfully obtained ohmic current-voltage characteristics, which are in good agreement with theoretical results within the framework of modified Anderson model. The calculated results also predict a high switching ratio in excess of 100000:1 for QC devices having the molecule sandwiched between the Ni electrodes, indicating that QC devices have potential application in novel switching devices.

Acknowledgements

This research has been partially supported by Special Education and Research Expenses from Post-Silicon Materials and Devices Research Alliance, a Grant-in-Aid for Young Scientists from The Ministry of Education, Culture, Sports, Science and Technology and Foundation Advanced Technology Institute (ATI). The authors would like to express their sincere appreciation to Dr. M. Hirasaka of Teijin Ltd., Research Manager K. Kubo of Teijin DuPont Films Japan Ltd., Prof. M. Yamamoto, Assist. Prof. K. Matsuda, Dr. S. Jin, H. Sato, M. Takei in Hokkaido University, Assoc. Prof. T. Komine in Ibaraki University and Prof. O. Kitakami in Tohoku University for helpful discussions.

References

[1] International Technology Roadmap for Semiconductors (ITRS) 2008 update
[2] Rothschild M, Bloomstein T M, Efremow Jr. N, Fedynyshyn T H, Fritze M, Pottebaum I and Switkes M 2005 *MRS Bulletin* **30** 942
[3] Roberts J, Bacuita T, Bristol R L, Cao H, Chandhok M, Lee S H, Leeson M, Liang T, Panning E, Rice B J, Shah U, Shell M, Yueh W and Zhang G J 2006 *Microelectron. Eng.* **83** 672
[4] Jung G Y, Halperin E J-, Wu W, Yu Z, Wang S -Y, Tong W M, Li Z, Green J E, Sheriff B A, Boukai A, Bunimovich Y, Heath J R and Williams R S 2006 *Nano Lett.* **6** 351
[5] Yu Z, Wu W, Jung G -Y, Olynick D L, Straznicky J, Li X, Li Z, Tong W M, Liddle J A, Wang S -Y and Williams R S 2006 *Nanotechnology* **17** 4956
[6] Kwon S, Yan X, Contreras A M, Liddle J A, Somorjai G A and Bokor J 2005 *Nano Lett.* **5** 2557
[7] Fujikawa S, Takaki R and Kunitake T 2006 *Langmuir* **22** 9057

[8] Ishibashi A 2004 *Proc. Int. Symp. on Nano Science and Technology* p.44
[9] Kaiju H, Ono A, Kawaguchi N and Ishibashi A 2008 *Jpn. J. Appl. Phys.* **47** 244
[10] Kondo K and Ishibashi A 2006 *Jpn. J. Appl. Phys.* **45** 9137
[11] Kondo K, Kaiju H and Ishibashi A 2008 *Mater. Res. Soc. Symp. Proc.* **1067** B0301
[12] Chen Y, Ohlberg D A A, Li X, Stewart D R, Williams R S, Jeppesen J O, Nielsen K A, Stoddard J F, Olynick D L and Anderson R 2003 *Appl. Phys. Lett.* **82** 1610
[13] Balzani V, Credi A, Mattersteig G, Matthews O A, Raymo F M, Stoddart J F, Venturi M, White A J P and Williams D J 2000 *J. Org. Chem.* **65** 1924
[14] Pease A R, Jeppesen J O, Stoddart J F, Luo Y, Collier C P and Heath J R 2001 *Acc. Chem. Res.* **36** 433
[15] Rahaman M D, Kaiju H, Kawaguchi N and A. Ishibashi 2008 *Jpn. J. Appl. Phys.* **47** 5712
[16] Ito E, Oji H, Furuta M, Ishii H, Oichi K, Ouchi Y and Seki K 1999 *Synthetic Metals* **101** 654
[17] Hirose Y, Kahn A, Aristov V and Soukiassian P 1996 *Appl. Phys. Lett.* **68** 217
[18] Tarlov M J, 1992 *Langmuir* **8** 80
[19] Nawate M, Shinohara K, Honda S and Tanaka H 2004 *Trans. Mater. Res. Soc. Jpn.* **29** 1599